Automatic Extraction of Mosaic Patterns in Uterine Cervix Images

Zhiyun Xue, L. Rodney Long, Sameer Antani, George R. Thoma
National Library of Medicine, National Institutes of Health
xuez@mail.nih.gov

Abstract

Mosaic vasculature is one crucial visual sign often indicating the existence of abnormality in the underlying cervix tissues. Automatic detection of this vascular pattern in uterine cervix images is a challenging task, especially in a large dataset, due to the factors such as fuzzy boundary, small vessel caliber, and appearance variation. In this paper, we present a supervised-learning based approach to segment the regions encompassing mosaic vasculatures, hoping to overcome these challenges. It is part of an automatic segmentation scheme that is aimed at assisting gynecologists in the study of cervical cancer. The affectivity of the method was tested and evaluated on a set of clinical uterine cervix images that were manually marked and categorized by medical experts.

1. Introduction

Cervigrams are color optical photos of uterine cervix taken following the application of 3-5% dilated acetic acid liquid. As a resemble of a low-magnified colposcopic photograph for providing an objective record of the cervix, the cervigram plays an important role not only in the medical diagnosis of cervical cancer, but also in the training of colposcopic assessment and the clinical research of the cancer. The National Library of Medicine (NLM) has been creating a large medical repository containing 100,000 cervigrams. These cervigrams were collected during two important cervical cancer research projects sponsored by the National Cancer Institute (NCI): the Guanacaste Project [1] and the ALTS Project [2]. The NLM cervigram collection is a great resource and has been utilized in various subprojects. One of the research interests is to identify visual characteristics of cervical neoplasia using automatic approaches. An internet-accessible cervigram segmentation tool, which incorporates extractions of multiple anatomical /medical landmarks on cervix, is under active development by our group. The interface of the tool is shown in Figure 1. This paper focuses on the segmentation of mosaic, one unique vasculature feature that is often associated with atypical cervical lesions.
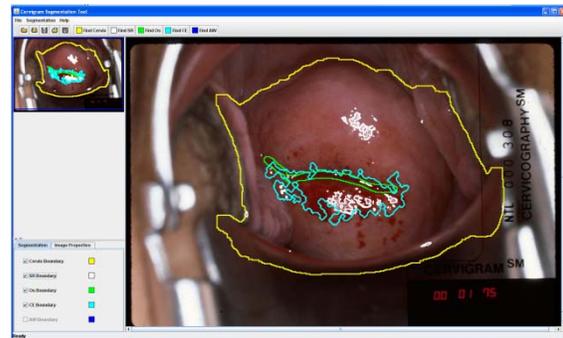

Figure 1. The Cervigram Segmentation Tool

Mosaic refers to a vascular pattern that is generated when inter-connecting capillaries are running parallel to the epithelium surface [3]. Visually, it appears as an irregular polygonal network encompassing various small, tile-like blocks, as shown in Figure 2. Mosaic patterns are of significance when they are found located on acetowhite epithelium. Acetowhite epithelium is a term for the areas becoming whitish after the application of acetic acid solution. It is a major visual sign observed in cervical neoplasia. Mosaic regions may be categorized as either fine or coarse. Fine mosaics refer to a network of thin-caliber capillaries that are closely interwoven. Coarse mosaics are a network composed of vessels with larger caliber and larger intercapillary distances. Fine mosaics tend to be associated with low grade lesions, while coarse mosaics tend to be found in lesions with more severe neoplasia.

Automatic segmentation of mosaic areas in NLM cervigram reservoir is a very challenging task due to the following attributing factors. First, there is a large appearance variation in the dataset due to the content variability and intensity inhomogenity. The shape, brightness, size and location of mosaic patterns vary

considerably across images. Second, the vessel calibers are usually small and the boundary between the mosaic structures and neighboring epithelium is fuzzy. Third, there are some noises and the mosaic patterns may coexist with other vasculatures, such as punctuations.
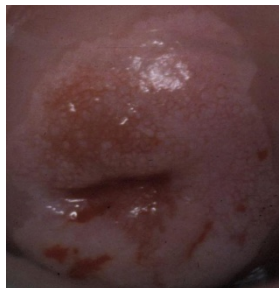

Figure 2. Mosaic pattern

In this paper, we propose a new approach for segmenting mosaic areas. It utilizes supervised learning techniques (using expert-annotated data), hoping to overcome those challenges. The expert-annotated data include the markings of acetowhite regions and mosaic subregions as well as the mosaic categories. They were collected through our in-house developed convenient tool, Boundary Marking Tool (BMT) [4]. In the following sections, we will present the details of the proposed method, the set of tools developed for it, and the experimental results.

2. Segmentation Methodology

In contrast to the approaches in [5-7], the proposed method circumvents the step of direct vascular structure extraction. The structure is difficult to be accurately segmented due to low contrast, fuzzy edge, small vessel caliber, and noise. To segment the mosaic areas, we split the input image into tiles; classify each tile as a mosaic tile or non-mosaic tile; and combine the classified tiles into a binary map. The method consists of four main blocks: pre-processing, feature extraction, supervised classification, and post-processing.

In pre-processing, the image is first cropped along the bounding box encompassing the expert-marked acetowhite regions to reduce the computational costs, since mosaics are vital signs only if they are confined to the acetowhite areas. Automatic detection of acetowhite regions are also under active development by our collaborated researchers [8-10]. Next, the small bright spots, named specular reflections (SR), are removed using the approach in [11]. It incorporates intensity, saturation and gradient information and utilizes probabilistic modeling to segment the reflection regions. These SR regions are then filled by

propagating the colors of surrounding non-SR pixels. The reason to remove these specular reflections is because the high gradients generated by these spots create texture-like patterns which may interfere the detection of mosaic patterns. Except the processing that is limited to SR regions, we avoid any other pre-processing, such as low-pass filtering and contrast enhancement, in order to preserve the vascular structure at most. The vague local contrast of mosaic vessels and the non-uniform color of mosaic vessels make the processing of low-pass filtering and contrast enhancement ineffective for the application. In fact, the low-pass filtering causes vessel boundaries less distinctive while contrast enhancement increases the effect of noises. Tiles of $M \times M$ image pixels are then extracted from the cropped image. These tiles are allowed to be overlapped by fifty percent with each other.

Each tile is treated as a binary classification problem, i.e., a classifier is applied to each tile to decide whether it is a mosaic tile or non-mosaic tile. To do that, four sets of features representing its texture information are calculated. To extract texture information, two grayscale images are considered. One is the green channel image, because the green channel shows the best vessel/background contrast compared to the red and blue channels when visualizing the RGB components of the color image separately. In colposcopy, doctors often use a green filter to assist their inspection of blood vessel patterns. The other is the luminance (Y') channel in the Y'UV color space. The Y' channel is produced by a weighted sums of R, G, and B channel ($Y' = 0.299R + 0.587G + 0.114B$ [12]), representing the brightness. Preliminary testing suggests the classification results using the Y' component of the color image are better. It might because the Y' component puts more weight on green channel but not discards the red and blue channels entirely. Therefore, the Y' channel was selected to be processed by texture descriptors. The features selected include:

- Gabor-Mean and Gabor-STD: This set of features is obtained by applying a Gabor filter bank to the tile image. The mean and standard deviation of the magnitude of the coefficients in filtered images are computed [13].
- Log-Gabor-Mean and Log-Gabor-STD: We also employ Log-Gabor filter to compensate limitations of the Gabor filter. Similarly, the mean and standard deviation of the magnitude of the transform coefficients are extracted [14].
- DWT-Mean and DWT-STD: They refer to the mean and standard deviation of the magnitude of the discrete wavelet decomposed images [15].

- GLCM-Contrast, GLCM-Correlation, GLCM-Energy, and GLCM-Homogeneity: The texture features related with gray-level co-occurrence matrix are considered too [16].

The features are normalized using the normal transformation in order to balance the unit disparity among different features. The normalization is applied separately to each image, hoping to compensate the illumination variations across the dataset. The vector formed by these features is then sent to the classifier.

Supervised classification is utilized based on expert-outlined mosaic regions. To create a labeled training set for tile classification, the samples are selected as follows. A tile that is completely enclosed by the expert-provided boundary of mosaic regions is chosen as a mosaic tile. A tile that does not belong to the expert-marked mosaic region but is located inside the expert-marked acetowhite region is selected as a non-mosaic tile. A non-linear support vector machine (SVM) is employed as the classifier because of its proved good performance on generalization [17]. Specifically, the Gaussian RBF kernel function is used and a procedure of v-fold cross-validation is applied for parameter selection (the C-SVC package of LIBSVM [18] is used).
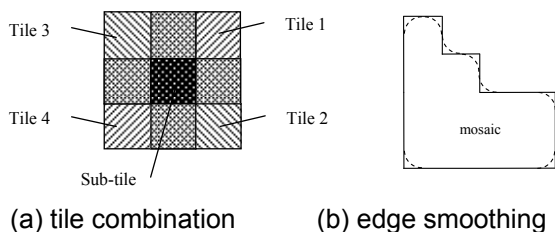

(a) tile combination   (b) edge smoothing

Figure 3. Post-processing

Given a new testing image, we first crop it and split it into tiles as described in the preprocessing step. For each testing tile, a feature vector is computed and normalized first. Then it is classified by the SVM classifier. The final segmentation map of the mosaic regions is obtained by combining the SVM-classified tiles. Because the tiles are fifty-percent overlapped with each other, for each sub-tile in the newly-formed segmentation map whose size is a quarter of the size of the tile, there are corresponding four tiles that enclose it, as illustrated in Figure 3(a), except those sub-tiles along the boundary of the map. All these tiles will be checked. If at least one of them is labeled as +1, then the sub-tile is set to be an all-one tile. If all of them are labeled as -1, then the sub-tile is set to be an all-zero tile. After obtaining this segmentation map with white area indicating the mosaic regions of interest (ROI), the following procedure is applied to further refine the map. As shown in Figure 3(b), the boundary of the segmented map is zig-zag due to the tile splitting and "piling" (placing tiles adjacently to form a connected region). To smooth out the zig-zags, we replace each corner of the region with a quarter circular arc of radius equal to a half of the width of the sub-tile. In implementation, it is done by applying the morphological transforms of opening followed by closing to the binary segmentation image using a disk-shaped structuring element. Next, the area outside the marked acetowhite regions is set to be non-mosaic region since the mosaics are significant only when they are found localized in the acetowhite areas. The isolated ROI whose area is too small (the size of the sub-tile) is removed.
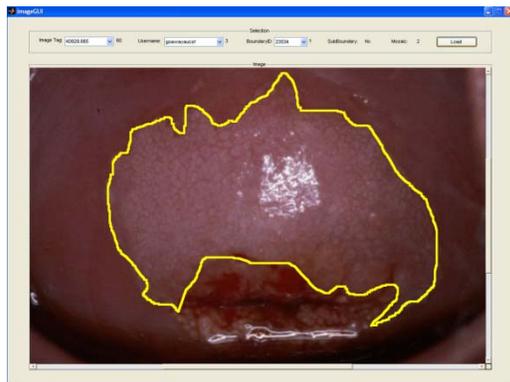
3. Experimental Results

3.1 Dataset

The image set that was under investigation contains images in which both the acetowhite region and its sub mosaic area were marked by at least one of the two experts using BMT. Only those agreed by both experts that there was mosaicism (one may not outline the region) was used, to lessen the problem of inter-observer variations that may cause possible ambiguities in classification. In addition, the union of the two corresponding regions was considered if both experts marked the boundary of it. As a result, the dataset consisted of 39 cervigrams. To divide the image into small tiles, the size of tiles need to be determined. It should be set large enough to capture the characteristics of mosaic patterns, but small enough to adapt to the shape and size variation of mosaicism. The typical size of the test color cervigrams is 2400×1640 pixels. The tile size was set to 64×64 pixels, which was found to adequately represent mosaic characteristics and result in good segmentation in experimental testing. The training group consisted of 19 cervigrams, which corresponded to 674 SVM positive training examples and 1789 SVM negative training examples. The number of negative training examples is more than twice that of positive training examples, which reflects and take into account that the diversity among non-mosaic areas is much larger than that among mosaic areas.
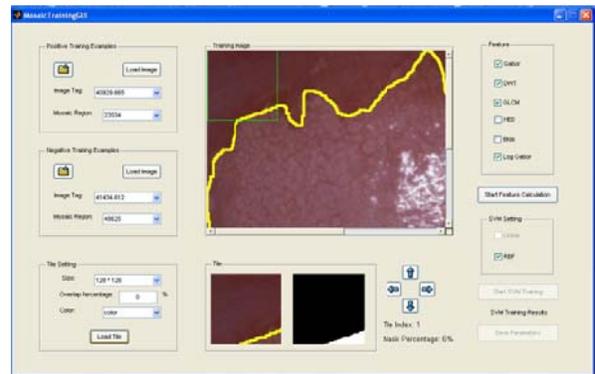
3.2 Mosaic analysis tools

To facilitate the analysis of mosaic patterns, a set of tools were implemented with MATLAB. They are the mosaic display tool, mosaic training tool, mosaic testing tool, and mosaic result tool. The mosaic display

tool (Figure 4(a)) is to assist the visual examination of all the regions containing mosaic patterns in the employed dataset. It shows the cropped image and the expert-marked mosaic region, along with the expert specified classification of the mosaic patterns. The mosaic training tool (Figure 4(b)) is to run the SVM training procedure. It allows a convenient setting of parameters used for training. Specifically, it contains panels for loading the training images, specifying parameters related with tile setting (size, and overlapping percentage), identifying the types of texture features to be used, and specifying the type of kernel functions used by the SVM classifier. Th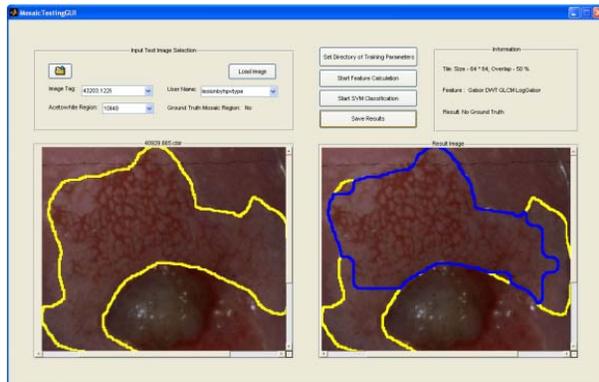e image and location of each extracted tile are also provided. The mosaic testing tool (Figure 4(c)) is to extract mosaicism given a new image. Using the same parameters specified in the training process, the test image will undergo the following procedure: it is split into tiles; each tile is labeled by the trained SVM classifier based on the texture features extracted from it; and the labeled tiles are integrated into a segmentation map. The automatic extracted mosaic area is then outlined on the image in blue color. The mosaic result tool (Figure 4(d)) is to facilitate the visual comparison of the automated segmentation results and the ones marked by experts.
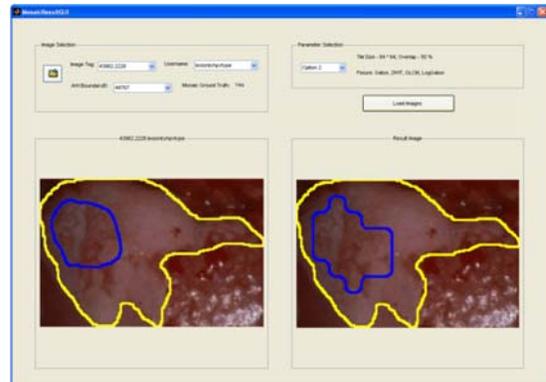

(a) mosaic display tool

(b) mosaic training tool
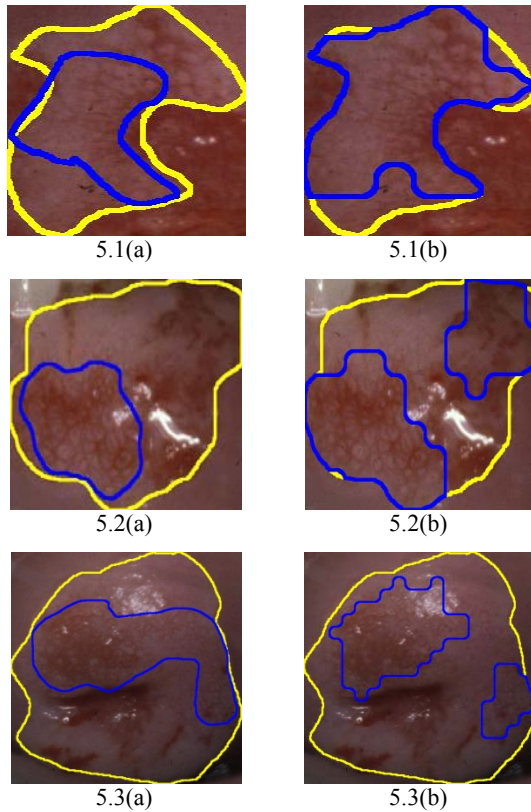

(c) mosaic testing tool

(d) mosaic result tool

Figure 4. Mosaic analysis tools

3.3 Evaluation

The segmentation performance was examined and compared to expert-based markings via visual inspection using the mosaic result tool. Overall, the proposed algorithm appears promising in identifying the areas where mosaics are located. Example results of testing images are presented in Figure 5. All the images were cropped along the periphery of the bounding box of acetowhite regions that are marked in yellow color. The mosaic regions are indicated with blue color. Each pair corresponds to a different acetowhite area, in which (a) shows the mosaic region marked by experts and (b) displays the region generated by the automatic segmentation method.

5.1(a)   5.1(b)

5.2(a)   5.2(b)

5.3(a)   5.3(b)

(a): mosaic areas marked by expert

(b): mosaic areas segmentated by the proposed method

Figure 5. Mosaic segmentation results

4. Conclusions and Future Work

This paper targets the detection of mosaicism in a large collection of cervicographic images. Mosaicism is one crucial vascular structure used by physicians to identify lesion abnormality. Automatic extraction of this important clinical feature in cervigrams is a difficult task, especially in this large image repository, due to their variation in shape, brightness, and size, and because of the noisy, blurred appearance of the mosaic structures. In this paper, we explored the potential benefit of a tile-based supervised classification approach for segmenting the regions exhibiting mosaic patterns. In the proposed approach, an SVM classifier was trained through supervised learning using expert-annotated region data and was applied to test each image tile whether it has mosaic patterns or not. One unique aspect of the proposed algorithm is that the stage of vascular structure extraction and skeletonization is avoided as opposed to previous mosaic detection methods. The performance of the proposed algorithm was evaluated using a set of 39

clinical cervigrams and the experimental results demonstrated its feasibility.

Several tasks have been identified for further improving the proposed mosaic segmentation algorithm. They include testing on a larger dataset, exploring a weighted SVM classifier, and investigating more features. For an algorithm based on supervised learning, the ground truth data is crucial to its development and assessment, which however is subject to the problem of intra- and inter- observer variability. To obtain a reliable ground truth dataset, the involvement of multiple medical experts is desired. We have been developing a tool called Multi-Observer Segmentation Evaluation System (MOSES) (Figure 6) [19]. Given a set of segmentations drawn by multiple raters, MOSES creates a probabilistic estimate of the true segmentation and evaluates the performance of the individual segmentation. We will use BMT and MOSES to gather more data and acquire high consensus ground truth dataset. In the SVM formulation we employed, the value of C, a penalty parameter that controls overfitting, is the same for both positive and negative classes. A cost-sensitive SVM method which assigns different weights to the errors of the two classes will be investigated. With regard to features, ten sets of texture features extracted using Gabor filters, Log-Gabor filters, DWT, and GLCM were utilized. More features are going to be explored.
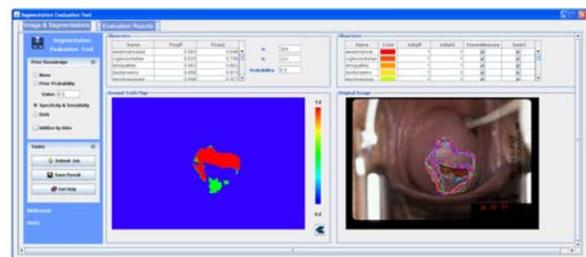

Figure 6. Interface of MOSES

References

[1] M. C. Bratti, A. C. Rodriguez, M. Schiffman, A. Hildesheim, J. Morales, M. Alfaro, D. Guillen, M. Hutchinson, M. E. Sherman, C. Eklund, J. Schussler, J. Buckland, L. A. Morera, F. Cardenas, M. Barrantes, E. Perez, T. J. Cox, R. D. Burk, R. Herrero, "Description of a seven-year prospective study of human

papillomavirus infection and cervical neoplasia among 10, 000 women in Guanacaste, Costa Rica", Revista Panamericana de Salud Pública/Pan American Journal of Public Health, vol. 15, no. 2, pp. 75–89, 2004.

[2] M. Schiffman, M. E. Adrianza, "ASCUS-LSIL Triage Study: Design, methods and characteristics of trial participants", Acta Cytologica, vol. 44, no. 5, pp.726–742, 2000.

[3] J.W. Sellors, R. Sankaranarayanan, "Colposcopy and Treatment of Cervical Intraepithelial Neoplasia - A Beginner's Manual", Edited by J.W. Sellors and R. Sankaranarayanan, Published by the International Agency for Research on Cancer, France, 2003.

[4] L. R. Long, S. Antani, G. R. Thoma, "Image informatics at a national research center", Computerized Medical Imaging and Graphics, vol. 29, pp. 171-193, February 2005.

[5] Q. Ji, J. Engel, E. Craine, "Texture analysis for classification of cervix lesions", IEEE Transactions on Medical Imaging, vol. 19, no. 11, pp. 1144-1149, 2000.

[6] W. Li, A. Poisson, "Detection and characterization of abnormal vascular patterns in automated cervical image analysis," Lecture Notes in Computer Science: Advances in Visual Computing, vol. 4292, pp. 627-636, 2006.

[7] Y. Srinivasan, F. Gao, B. Tulpule, S. Yang, S. Mitra, and B. Nutter, "Segmentation and classification of cervix lesions by pattern and texture analysis", International Journal of Intelligent Systems Technologies and Applications, vol.1, no.3, pp. 234-246, 2006

[8] A. Alush, H. Greenspan, J. Goldberger, "Lesion detection and segmentation in uterine cervix images using an arc-level MRF", Proceedings of IEEE International Symposium on Biomedical Imaging, pp. 474-477, 2009

[9] X. Huang, W. Wang, Z. Xue, S. Antani, L. R. Long, J. Jeronimo, "Tissue classification using cluster features for lesion detection in digital cervigrams", Proceedings of SPIE Medical Imaging, vol. 6914, pp. 69141Z-1-8, February 2008

[10] H. Greenspan, S. Gordon, G. Zimmerman, S. Lotenberg, J. Jeronimo, S. Antani, R. Long. "Automatic detection of anatomical landmarks in uterine cervix images", IEEE Transactions on Medical Imaging, vol. 28, no.3, pp. 454-68, 2009.

[11] G. Zimmerman, H. Greenspan, "Automatic detection of specular reflections in uterine cervix images", Proceedings of SPIE Medical Imaging, vol. 6144, pp. 2037-2045, 2006

[12] J. C. Russ, The Image Processing Handbook, ISBN 0849372542, 2006.

[13] B. S. Manjunath, W. Y. Ma, "Texture features for browsing and retrieval of image data", IEEE Trans Pattern Analysis and Machine Intelligence, vol. 18, no. 8, pp. 837-842, 1996.

[14] D. J. Field. "Relations between the statistics of natural images and the response properties of cortical cells", Journal of Optical Society of America, pp. 2379-2394, 1987.

[15] M. N. Do, M. Vetterli, "Wavelet-based texture retrieval using generalized Gaussian density and Kullback-Leibler distance", IEEE Transactions on Image Processing, vol. 11, no. 2, pp. 146-158, 2002

[16] R. Haralick, K. Shanmugam, I. Dinstein, "Texture features for image classification", IEEE Transactions on Systems, Man and Cybernetics, vol. 3, pp. 610-621, 1973.

[17] C. J. C. Burges, "A tutorial on support vector machines for pattern recognition", Data Mining and Knowledge Discovery, vol. 2, no.2, pp.121–167, 1998.

[18] C. Chang, C. Lin, "LIBSVM: a library for support vector machines", 2001. Software available at http://www.csie.ntu.edu.tw/~cjlin/libsvm.

[19] Y. Zhu, W. Wang, X. Huang, D. Lopresti, L. R. Long, S. Antani, Z. Xue, G. Thoma, "Balancing the role of priors in multi-observer segmentation evaluation", Journal of Signal Processing Systems, vol. 55, no. 1-3, pp. 158-207, May 2008.